Letter

Temporal light control in complex media through the singular-value decomposition of the time-gated transmission matrix

Louisiane Devaud,[1,*] Bernhard Rauer,[1] Matthias Kühmayer,[2] Jakob Melchard,[2]
Mickaël Mounaix,[1,3] Stefan Rotter,[2] and Sylvain Gigan[1]

[1]*Laboratoire Kastler Brossel, ENS-Université PSL, CNRS, Sorbonne Université, Collège de France, 24 rue Lhomond, 75005 Paris, France*
[2]*Institute for Theoretical Physics, Vienna University of Technology (TU Wien), A-1040 Vienna, Austria*
[3]*School of Information Technology and Electrical Engineering, The University of Queensland, Brisbane, QLD 4072, Australia*

(Received 4 February 2022; accepted 21 April 2022; published 10 May 2022)

The complex temporal behavior of an ultrashort pulse of light propagating through a multiple scattering medium can be characterized experimentally through a time-gated transmission matrix. Using a spatial light modulator, we demonstrate here that injecting singular vectors of this matrix allows us to optimally control the energy deposition at any controllable delay time. Our approach provides insights into the fundamental aspects of multispectral light scattering and could find applications in imaging or coherent control.

DOI: 10.1103/PhysRevA.105.L051501

A coherent light pulse passing through a multiple scattering medium gets distorted into speckled interference patterns—both in space and time [1]. Even though the resulting pattern is seemingly random, it results from linear and deterministic scattering events and can therefore be controlled [2]. In recent years, many techniques have been developed enabling the control of the scattered light by means of shaping the input field [3,4].

A concept that enables a particularly detailed control of light propagation through scattering media is the transmission matrix (TM) [5]. For a given wavelength, the monochromatic TM relates the light field entering the medium to the output field, thus encoding the entire transmission behavior of the scattering sample. Once measured, an "inversion" of this matrix thus enables the focusing at arbitrary locations, the transmission of images [6], as well as the creation of states that are invariant to scattering [7]. In addition, decomposing the matrix in its eigen- or singular modes gives access to orthogonal input channels sorted by their total transmission [8,9]. This is not only interesting for the study of mesoscopic effects, accessible when measuring a large fraction of the modes, such as open and closed channels [10–12], but also for controlling the overall transmission and reflection of a sample [13–15].

In the case of pulsed illumination, the speckled interference pattern acquires an additional temporal component as the different wavelengths of the pulse propagate differently in the scattering process [16]. The TM concept still holds in this situation but needs to be extended to a multispectral TM, encoding the transmission of each spectral channel [17]. The number of distinct spectral channels needed to capture the full transmission behavior depends on the scattering sample and on the bandwidth of the input pulse. In order to address the light arriving at a certain time, one can either Fourier transform a multispectral TM [18,19] or directly perform a time-resolved measurement, resulting in a time-gated TM which is valid only for a certain arrival time in the scattered pulse. This tool already proved useful for spatiotemporal focusing behind scattering media [20], for focusing on an object embedded inside a scattering sample [21], and, more recently, to control the energy delivery after propagation in a multimode fiber [18,19]. The two latter studies, however, only indirectly measure and manipulate the pulse response by measuring its individual monochromatic components and by reconstructing it in postprocessing.

In this Letter, we report on the temporal control of a femtosecond laser pulse that passes through a multiple scattering medium. We characterize the scattering process through the direct measurement of the time-gated TM by interfering the scattered light with a controllable delayed probe pulse. Performing the singular-value decomposition (SVD) of this time-gated TM provides us with a set of input modes that enable temporal control, beyond simple focusing [20]. Through direct measurements of the time-resolved transmission, we are able to show that the singular vectors of the time-gated TM can be used to enhance or diminish the energy arriving at any selected time in the output pulse, enabling a smooth and accurate control of the temporal intensity distribution. We complement our experimental observations with simulations of scattering waveguides that allow us to probe regimes of control not easily accessible experimentally. In this way we uncover the existence of states that are perfectly nontransmitting at given delay times in the output pulse. Working with the SVD has the advantage of accessing the state with *optimal* transmission at any given time—a feature recently addressed in the context of monochromatic light [8], broadband inputs in optical fibers [18,19], the deposition matrix [22], or non-normal photonic media [23]. We illustrate this aspect by comparing the SVD states to other strategies to enhance the total transmission. To illustrate the versatility of the SVD-based transmission control, we show how to use it for controlling the speckle grain size at a specific time [24].

*louisiane.devaud@lkb.ens.fr

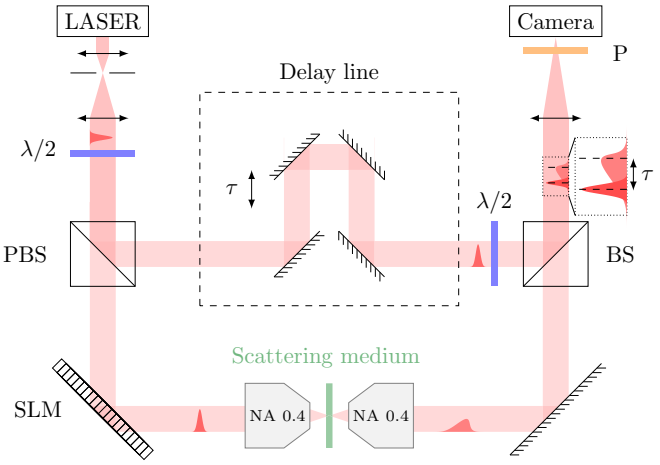

FIG. 1. Scheme of the experimental setup. An ultrashort pulse of light, of central wavelength $\lambda_0 = 808$ nm, delivered from a Ti:sapphire pulsed laser (MaiTai HP, Spectra Physics, $\simeq$100 fs pulse length) is divided upon two paths by a polarizing beam splitter (PBS). On one path the pulse wavefront is modulated by a reflective phase-only SLM (HSP512L-1064, Meadowlarks) and passes through a $\sim$10 µm scattering layer of TiO_2 particles (transmittance of $\sim$0.3, suspended on a glass slide and static on the timescale of experiments) where it gets elongated. On the second path, the pulse is sent on a controlled delay line. Both pulses get recombined on a beam splitter (BS) and are imaged on a CCD camera (Manta, G-046, Allied Vision). Two half-wave plates ($\lambda/2$) adjust the polarization of the power of both arms and a polarizer (P) before the camera selects the desired polarization.

The experimental setup used is sketched in Fig. 1. An ultrashort pulse of light, modulated by a reflective phase-only spatial light modulator (SLM), is sent through a slab of scattering material. Multiple scattering processes elongate the pulse in time before it is imaged on a charged coupled device (CCD) camera. Additionally, an unperturbed plane-wave probe pulse, decoupled from the beam before the SLM, is recombined and interferes with the scattered light at the CCD. A delay line in the probe path allows us to tune the time delay τ between the scattered light and the probe pulse. Scanning the probe pulse delay over the elongated pulse enables us to retrieve the spatiotemporal field of the scattered light [20,25] (for more details, refer to Supplemental Material (SM) [26] Secs. I and II).

This time-gated configuration enables us to measure a time-gated TM at any desired delay time τ_0 within the distribution of delays induced by the scattering. To this end, a set of orthogonal spatial modes (Hadamard basis) is displayed on the SLM while for each mode the output field is measured on the CCD by phase stepping the pattern on the SLM between 0 and 2π [5]. As the probe pulse only interferes with the part of the scattered light that matches its delay, the measured TM only encodes information about this given delay. The rest of the light acts as a background and does not influence the TM measurement.

Using phase conjugation, it has already been shown that the information contained in the TM can be used to concentrate light at single or multiple spatiotemporal positions [20]. Here, instead, we address the question of how to achieve the globally optimal energy delivery in a selected output region, at a predetermined time τ_0. The method of choice for this task is to perform an SVD of the time-gated TM, which yields the real singular values s_i and the orthogonal input singular vectors v_i associated with them (see SM [26] Sec. III.). The number of nonzero singular values at a given time τ_0 corresponds to the matrix rank and we sort them in decreasing order. Correspondingly, the first singular vector v_1 corresponds to the largest singular value and thus to the globally optimal transmission at the time delay τ_0. In the experiment, we display the phase of the singular vectors on the SLM and record the resulting output pulses. The impact of a specific input wavefront on the temporal shape of the output is measured by tuning the delay of the probe pulse over the full extended duration of the scattered pulse while recording their interference. In Fig. 2(a) we present the temporal shape of the scattered field amplitude, spatially averaged over the full area over which the time-gated TM was measured for two of its singular vectors. The first singular vector v_1, associated with the highest singular value, leads to a sharp increase of the field amplitude in the region of interest at τ_0. On the contrary, the last singular vector v_{225} ($N_{\mathrm{CCD}} = 225$), associated with the lowest singular value, results in a decrease at that delay τ_0. Outside of the controlled time bin, the temporal profile of the pulse is not affected. The temporal width of the affected region is larger than the original pulse width due to the homodyne measurement process—its value is detailed in SM [26] Sec. IV.

These two singular vectors represent the extreme cases of field enhancement or reduction. Sending singular vectors associated to intermediate singular values enables us to tune the enhancement to field values in between [see the inset of Fig. 2(a)]. Here, we define the amplitude increase ratio η_{E} as the relative enhancement, at the target time, of the field amplitude relative to the unshaped plane-wave input pulse. The measured enhancement values follow qualitatively the TM singular-value distribution. The observed discrepancy in magnitude of the enhancement can be explained by the phase-only constraint of our wavefront modulation while the global shape is reproduced well by a random matrix model (see SM [26] Sec. VI). The singular vector spectrum of the time-gated TM hence enables smooth control of the energy delivery at the target time τ_0.

Through measuring the time-gated TM for different delay times, temporal control can be gained over the whole duration of the elongated pulse, as shown in Fig. 2(b) for the first singular vector. Yet, its effectiveness depends on the value of τ_0, with the increase ratio reaching a maximum at around $\tau_0 \approx 1.1$ ps which corresponds to about double the Thouless time of the medium [27]. The decay of the enhancement for late times can be attributed to a drop in the signal-to-background ratio of the TM measurement (in line with related observations in Ref. [28]). Our work also shows that the delay at which the energy variations apply can slightly differ from τ_0, especially for short and long delays (see SM [26] Sec. VI).

Up to now, we demonstrated control of the global pulse amplitude at a single delay time only. However, to gain control over multiple times at once, linearity enables us to sum the singular vectors associated to time-gated TMs measured at different times, as presented in Fig. 2(c). This is analogous to the superposition of multiple spatial, spatiotemporal, or

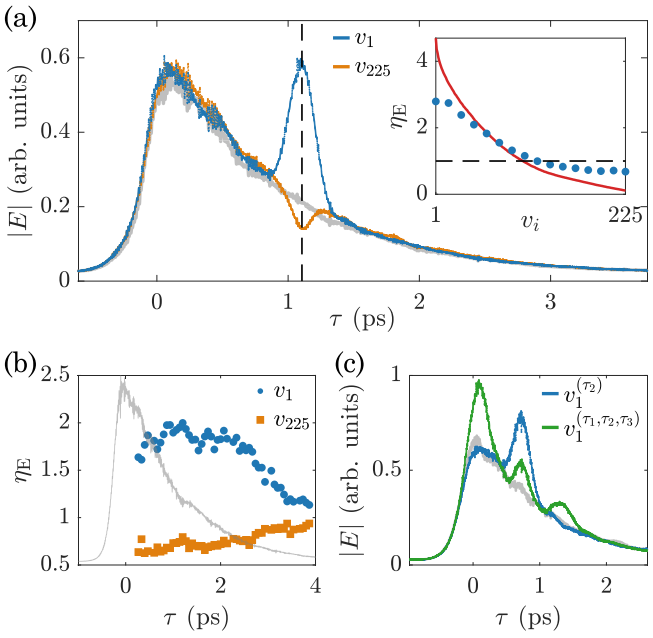

FIG. 2. Temporal control of scattered light with the time-gated TM. (a) Temporal profile of the spatially averaged output pulse amplitude $|E|$ for the first singular vector v_1 (peaked blue) and the last singular vector v_{225} (dented orange) of a time-gated TM measured at $\tau_0 = 1.1$ ps. The pulse shape obtained for a plane-wave input is shown in gray. In the inset, the amplitude enhancement η_E (measured at τ_0) relative to the plane-wave input is shown for the whole range of singular vectors (blue dots). The expected field enhancement for phase and amplitude control $\tilde{s} = s/\sqrt{\langle s^2 \rangle}$ corresponds to the normalized singular values (see SM [26] Sec. VI.) and is indicated by the red solid line. (b) Enhancements obtained with the first (v_1, blue dots) and last (v_{225}, orange squares) singular vectors for different delay times τ_0. The plane-wave output pulse is shown as a visual aid (arbitrary units, gray line). Here, the individual time-gated TMs have been measured with ten phase steps per mode (instead of four—see SM [26] Sec. I) to reduce measurement noise in the pulse tail. (c) Simultaneous enhancement at three different delay times by projecting the sum of the corresponding TM's first singular vectors $v_1^{(\tau_1,\tau_2,\tau_3)}$ (three peaks, green) compared to the plane-wave input (no peaks, gray) and to a single time control $v_1^{(\tau_2)}$ (single peak, blue). All TMs used here were measured for $N_{\mathrm{SLM}} \simeq 640$ (see SM [26] Sec. III A) and $N_{\mathrm{CCD}} = 225$. Data displayed in (a) are averaged over four disorder realizations whereas (b) and (c) correspond to a single realization.

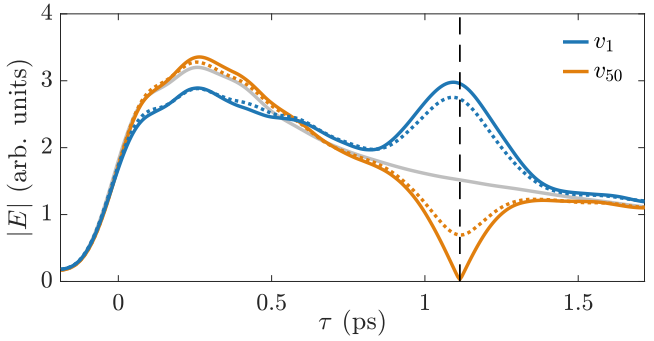

FIG. 3. Simulation results in a waveguide geometry with a similar scattering strength and using 50 input and output modes. Solid lines indicate the output pulse shapes for amplitude and phase control of the singular vectors v_1 (peaked blue) and v_{50} (dented orange) corresponding to the largest and smallest singular value of the TM at the value of τ_0 (indicated by the vertical dashed black line). The corresponding results for phase-only control are depicted by dashed lines. The gray line represents the time-of-flight reference when injecting a set of random inputs. The simulation results are averaged over ten realizations of the disorder.

spatiochromatic foci [5,17,20,29]. As for the spatial superpositions, tuning the pulse amplitude at multiple times with a single SLM mask naturally leads to a drop in efficiency.

An important technical limitation in our setup is the restriction to phase-only input patterns. Even though the singular vectors contain the amplitude information, we only project their phase on the SLM. In order to better understand how this limitation affects the temporal shaping presented, we turn to simulations. For a two-dimensional waveguide geometry filled with randomly placed obstacles we solve the scalar Helmholtz equation for 50 transverse input and output modes (for details, see SM [26] Sec. V). Doing this for a range of wavelengths we can retrieve the temporal response of the waveguide through a Fourier transform [18,19]. This provides us with the time-resolved TM, allowing us to calculate its SVD and to evaluate the output pulse shape for different input singular vectors. Figure 3 shows the response for the extremal vectors v_1 and v_{50}, both for phase and amplitude and phase-only control. For the latter, we find good qualitative agreement with the experimental results. As expected, the additional amplitude control yields a larger modulation of the field at the target delay (indicated by the vertical dashed black line). In the case of the first singular vector, however, the difference between full control and phase-only control is not large. For the last singular vector, on the other hand, the additional amplitude control allows us to create a zero crossing of the electric field (in line with results obtained in multimode fibers where a quasicancellation of the field was observed [19]).

Note that, in the waveguide, the fraction of modes that is controlled is limited to the lowest 50% (see SM [26] Sec. V), whereas in the experiment a much smaller fraction of all modes is controlled. In addition, the transverse boundary conditions differ. The good agreement between the simulation and the experimental results is therefore all the more striking and indicates that SVD-based temporal control is a widely applicable tool.

In the following, we compare our SVD control to conceptually simpler strategies to enhance the energy at a certain time. A spatiotemporal focus, for example, also leads to a temporal focus, albeit only at a single location [20]. For the light to be focused on several locations at once, many focusing wavefronts can be superposed at the cost of a lower enhancement for the individual foci. Contrary to what one might expect, focusing simultaneously on each output pixel for which the TM was measured does not entirely diminish the overall enhancement of the delivered light (see SM [26] Sec. VI). This global-focus pattern can be obtained by simply summing the time-gated TM over all output elements. A comparison of the field enhancement obtained from the

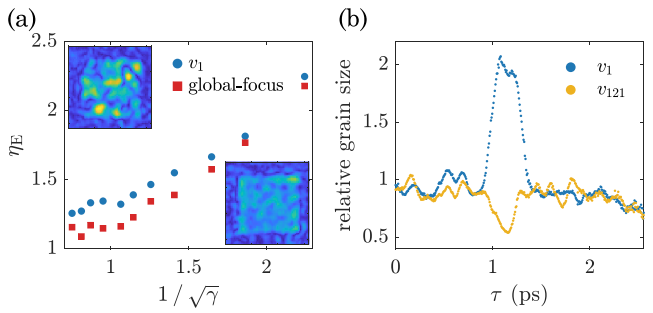

FIG. 4. (a) Amplitude enhancement η_E over the degree of control scaled as $1/\sqrt{\gamma}$ for the first singular vector v_1 (blue dots) and the global-focusing vector (red squares). Here, $N_{SLM} \simeq 120$ was fixed and N_{CCD} was varied from $N_{CCD} = 25$ $(1/\sqrt{\gamma} = 2.25)$ to $N_{CCD} = 225$ $(1/\sqrt{\gamma} = 0.75)$. The insets show typical examples of the output field amplitude patterns for the first singular vector (top left) and the global-focusing vector (bottom right). Output fields are only affected in the region where the TM was measured, a central square, and the edges are displayed for visual reference. (No average over disorder realizations was performed.) (b) Temporal evolution of the speckle grain size for the first singular vector v_1 (peaked blue) and an intermediate singular vector v_{121} (dented yellow) in the same configuration used in Figs. 2(a) and 2(b). At each τ the speckle grain size is normalized to the one obtained for the plane-wave input pulse. For all data presented in this figure the TM was measured at $\tau_0 = 1.1$ ps. (An average over four disorder realizations was performed.)

global focus and the first singular vector for different degrees of control $\gamma = N_{CCD}/N_{SLM}$ is presented in Fig. 4(a). We see that for a large number of output modes $(1/\sqrt{\gamma} \leqslant 1)$ the SVD has a distinct advantage while in the case of few output pixels $(1/\sqrt{\gamma} \gg 1)$ the global focus leads to similar temporal enhancements. In the extreme case of a single output pixel the first singular vector and the global-focus pattern are naturally equivalent [30]. The scaling of the enhancement with $1/\sqrt{\gamma}$ is predicted analytically (see SM [26] Sec. VI B).

The smaller enhancements of the global-focus input compared to the first singular vector is expected since the summation of all TM rows constrains the field on all output pixels to have the same phase and amplitude values. This restriction prevents the optimally transmitting mode from being reached and leads to non-Rayleigh distributed output patterns. The insets in Fig. 4(a) illustrate this by comparing the global-focus output to the Rayleigh distributed output speckle obtained with the first singular vector (see also SM [26] Sec. VII).

To demonstrate the versatility of working with singular vectors of the time-gated TM, we show here how this approach can also be used to control speckle correlations at well-defined moments in time. For this purpose we translate a technique originally introduced for oversampled monochromatic TMs [24] to the temporal domain. Relying on an imbalance in the transmission of different spatial frequencies encoded in the TM, this technique enables the control of the speckle grain size through a selection of different singular vectors. For the time-gated TM, this effect translates to the time domain, allowing for a temporal control of the speckle grains as shown in Fig. 4(b). The grain size variations over the pulse are presented for two singular vectors and in analogy to the monochromatic case they can be tuned continuously when utilizing the full spectrum of singular vectors. We expect these results to trigger more advanced temporal correlation engineering in complex media.

In conclusion, we present an experimental technique based on the SVD of the time-gated TM which enables the temporal control of the global light delivery on the region of interest through a complex scattering medium. By selecting different singular vectors as inputs we can continuously tune the transmission of a laser pulse at the desired arrival times. Such pulse-shaping capabilities might be useful for pump-probe experiments or for nonlinear excitations through scattering environments. Moreover, we observe in simulations that amplitude and phase control at the input should allow for a perfect cancellation of the output field at a desired point in time. To further match experiments, performing a three-dimensional simulation, as presented in Ref. [31], would be of interest. We also compare the SVD-based transmission enhancement with a global-focusing approach that also boosts transmission, but falls short in efficiency and yields different output speckle statistics. The preservation of Rayleigh statistics with the SVD may be an asset for speckle-based imaging techniques such as speckle-field digital holography microscopy [32] or for blind structured illumination microscopy [33]. An important point to stress is that, compared to previous studies that investigated temporal power enhancements in multimode fibers [18,19], we perform measurements directly in the time domain. Instead of measuring the full monochromatic response of the system and calculating the anticipated temporal response by means of a Fourier transformation, we work with pulsed light and time-gated measurements. This means we only need a minimal number of measurements to shape the temporal light distribution, allowing us to explore interactions with nonlinear processes in the future. Note that enlarging the formalism to nonlinear problems, such as random laser peak tuning [34] for instance, even though not evident, would be interesting. For now our results will further improve the understanding of the time-gated TM and the fundamental possibilities of spatiotemporal light shaping in complex scattering environments.

This project was funding by the European Research Council under the Grant Agreement No. 724473 (SMARTIES), the European Union's Horizon 2020 research and innovation program under the Marie Skłodowska-Curie Grant Agreement No. 888707 (DEEP3P), and the Austrian Science Fund (FWF) under Project No. P32300 (WAVELAND). The computational results presented in this Letter were achieved using the Vienna Scientific Cluster (VSC). M.M. acknowledges funding from the Australian Research Council (DE210100934).

[1] J. Goodman, *Speckle Phenomena in Optics: Theory and Applications* (Roberts & Company, Greenwood Village, CO, 2007).

[2] I. M. Vellekoop and A. Mosk, Focusing coherent light through opaque strongly scattering media, Opt. Lett. **32**, 2309 (2007).

[3] A. P. Mosk, A. Lagendijk, G. Lerosey, and M. Fink, Controlling waves in space and time for imaging and focusing in complex media, Nat. Photonics **6**, 283 (2012).

[4] S. Rotter and S. Gigan, Light fields in complex media: Mesoscopic scattering meets wave control, Rev. Mod. Phys. **89**, 015005 (2017).

[5] S. M. Popoff, G. Lerosey, R. Carminati, M. Fink, A. C. Boccara, and S. Gigan, Measuring the Transmission Matrix in Optics: An Approach to the Study and Control of Light Propagation in Disordered Media, Phys. Rev. Lett. **104**, 100601 (2010).

[6] S. Popoff, G. Lerosey, M. Fink, A. C. Boccara, and S. Gigan, Image transmission through an opaque material, Nat. Commun. **1**, 81 (2010).

[7] P. Pai, J. Bosch, M. Kühmayer, S. Rotter, and A. P. Mosk, Scattering invariant modes of light in complex media, Nat. Photonics **15**, 431 (2021).

[8] M. Kim, Y. Choi, C. Yoon, W. Choi, J. Kim, Q.-H. Park, and W. Choi, Maximal energy transport through disordered media with the implementation of transmission eigenchannels, Nat. Photonics **6**, 581 (2012).

[9] H. Yu, T. R. Hillman, W. Choi, J. O. Lee, M. S. Feld, R. R. Dasari, and Y. K. Park, Measuring Large Optical Transmission Matrices of Disordered Media, Phys. Rev. Lett. **111**, 153902 (2013).

[10] O. Dorokhov, On the coexistence of localized and extended electronic states in the metallic phase, *30 Years of the Landau Institute—Selected Papers* (World Scientific, Singapore, 1996), pp. 234–237.

[11] J. Pendry, A. MacKinnon, and A. Pretre, Maximal fluctuations—a new phenomenon in disordered systems, Physica A **168**, 400 (1990).

[12] C. W. Beenakker, Random-matrix theory of quantum transport, Rev. Mod. Phys. **69**, 731 (1997).

[13] I. M. Vellekoop and A. P. Mosk, Universal Optimal Transmission of Light Through Disordered Materials, Phys. Rev. Lett. **101**, 120601 (2008).

[14] B. Gérardin, J. Laurent, A. Derode, C. Prada, and A. Aubry, Full Transmission and Reflection of Waves Propagating through a Maze of Disorder, Phys. Rev. Lett. **113**, 173901 (2014).

[15] C. W. Hsu, S. F. Liew, A. Goetschy, H. Cao, and A. D. Stone, Correlation-enhanced control of wave focusing in disordered media, Nat. Phys. **13**, 497 (2017).

[16] D. J. McCabe, A. Tajalli, D. R. Austin, P. Bondareff, I. A. Walmsley, S. Gigan, and B. Chatel, Spatio-temporal focusing of an ultrafast pulse through a multiply scattering medium, Nat. Commun. **2**, 447 (2011).

[17] D. Andreoli, G. Volpe, S. Popoff, O. Katz, S. Grésillon, and S. Gigan, Deterministic control of broadband light through a multiply scattering medium via the multispectral transmission matrix, Sci. Rep. **5**, 10347 (2015).

[18] W. Xiong, C. W. Hsu, and H. Cao, Long-range spatio-temporal correlations in multimode fibers for pulse delivery, Nat. Commun. **10**, 2973 (2019).

[19] M. Mounaix and J. Carpenter, Control of the temporal and polarization response of a multimode fiber, Nat. Commun. **10**, 5085 (2019).

[20] M. Mounaix, H. Defienne, and S. Gigan, Deterministic light focusing in space and time through multiple scattering media with a time-resolved transmission matrix approach, Phys. Rev. A **94**, 041802(R) (2016).

[21] S. Jeong, Y.-R. Lee, W. Choi, S. Kang, J. H. Hong, J.-S. Park, Y.-S. Lim, H.-G. Park, and W. Choi, Focusing of light energy inside a scattering medium by controlling the time-gated multiple light scattering, Nat. Photonics **12**, 277 (2018).

[22] N. Bender, A. Yamilov, A. Goetschy, H. Yılmaz, C. W. Hsu, and H. Cao, Depth-targeted energy delivery deep inside scattering media, Nat. Phys. **18**, 309 (2022).

[23] K. G. Makris, L. Ge, and H. E. Türeci, Anomalous Transient Amplification of Waves in Non-normal Photonic Media, Phys. Rev. X **4**, 041044 (2014).

[24] L. Devaud, B. Rauer, J. Melchard, M. Kühmayer, S. Rotter, and S. Gigan, Speckle Engineering through Singular Value Decomposition of the Transmission Matrix, Phys. Rev. Lett. **127**, 093903 (2021).

[25] Z. Yaqoob, D. Psaltis, M. S. Feld, and C. Yang, Optical phase conjugation for turbidity suppression in biological samples, Nat. Photonics **2**, 110 (2008).

[26] See Supplemental Material at http://link.aps.org/supplemental/10.1103/PhysRevA.105.L051501 for experimental details and definitions, analytical results, and explanations of the waveguide simulation, which includes Refs. [1,5,24,35–40].

[27] D. J. Thouless, Maximum Metallic Resistance in Thin Wires, Phys. Rev. Lett. **39**, 1167 (1977).

[28] J. Aulbach, B. Gjonaj, P. M. Johnson, A. P. Mosk, and A. Lagendijk, Control of Light Transmission through Opaque Scattering Media in Space and Time, Phys. Rev. Lett. **106**, 103901 (2011).

[29] M. Mounaix, D. Andreoli, H. Defienne, G. Volpe, O. Katz, S. Grésillon, and S. Gigan, Spatiotemporal Coherent Control of Light through a Multiple Scattering Medium with the Multispectral Transmission Matrix, Phys. Rev. Lett. **116**, 253901 (2016).

[30] I. M. Vellekoop and A. Mosk, Phase control algorithms for focusing light through turbid media, Opt. Commun. **281**, 3071 (2008).

[31] A. Yamilov, S. E. Skipetrov, T. W. Hughes, M. Minkov, Z. Yu, and H. Cao, Anderson localization of electromagnetic waves in three dimensions, arXiv:2203.02842.

[32] Y. Park, W. Choi, Z. Yaqoob, R. Dasari, K. Badizadegan, and M. S. Feld, Speckle-field digital holographic microscopy, Opt. Express **17**, 12285 (2009).

[33] E. Mudry, K. Belkebir, J. Girard, J. Savatier, E. Le Moal, C. Nicoletti, M. Allain, and A. Sentenac, Structured illumination microscopy using unknown speckle patterns, Nat. Photonics **6**, 312 (2012).

[34] M. Leonetti and C. López, Active subnanometer spectral control of a random laser, Appl. Phys. Lett. **102**, 071105 (2013).

[35] A. Monmayrant, S. Weber, and B. Chatel, A newcomer's guide to ultrashort pulse shaping and characterization, J. Phys. B: At., Mol. Opt. Phys. **43**, 103001 (2010).

[36] M. Davy, Z. Shi, and A. Z. Genack, Focusing through random media: Eigenchannel participation number and intensity correlation, Phys. Rev. B **85**, 035105 (2012).

[37] S. Rotter, J.-Z. Tang, L. Wirtz, J. Trost, and J. Burgdörfer, Modular recursive Green's function method for ballistic quantum transport, Phys. Rev. B **62**, 1950 (2000).

[38] F. Libisch, S. Rotter, and J. Burgdörfer, Coherent transport through graphene nanoribbons in the presence of edge disorder, New J. Phys. **14**, 123006 (2012).

[39] R. Pierrat, P. Ambichl, S. Gigan, A. Haber, R. Carminati, and S. Rotter, Invariance property of wave scattering through disordered media, Proc. Natl. Acad. Sci. USA **111**, 17765 (2014).

[40] M. Davy, M. Kühmayer, S. Gigan, and S. Rotter, Mean path length invariance in wave-scattering beyond the diffusive regime, Commun. Phys. **4**, 85 (2021).